CHEMMEDCHEM

DOI: 10.1002/cmdc.201100199

Bis[3,5-bis(benzylidene)-4-oxo-1-piperidinyl]amides: A Novel Class of Potent Cytotoxins

Swagatika Das,[a] Umashankar Das,[a] Armando Varela-Ramírez,[b] Carolina Lema,[b] Renato J. Aguilera,[b] Jan Balzarini,[c] Erik De Clercq,[c] Stephen G. Dimmock,[d] Dennis K. J. Gorecki,[a] and Jonathan R. Dimmock*[a]

The principal objective of this study was the examination of the theory of cytotoxic synergism. In this exploratory study, we tested the hypothesis that doubling the number of sites available for thiol alkylation in a series of candidate cytotoxins increases potency more than two-fold. This concept was verified in one-third of our comparisons using human Molt 4/C8 and CEM T-lymphocytes and murine L1210 cells. In addition, the significant potencies of various members of our compound series justified further studies. Molecular modeling revealed that relative locations of the amidic groups correlate with cytotoxicity. A potent cytotoxic compound, 1,2-bis(3,5-dibenzylidene-4-oxo-piperidin-1-yl)ethane-1,2-dione (**1a**) inhibited the growth of a large number of human tumor cell lines and displayed greater toxicity toward certain non-adherent cells than toward adherent neoplasms or fibroblasts. The mode of action of **1a** includes induction of apoptosis and necrosis.

Introduction

The principal aim of this work was the design, syntheses, and biological evaluation of conjugated styryl ketones as candidate antineoplastic agents. A number of studies have revealed that these enones react readily with thiols.[1,2] In particular, conjugated styryl ketones react only with the thiol group in a variety of compounds containing other functional groups such as amino,[3] and hydroxy groups,[4] as well as with proteins containing one or more mercapto substituents.[5] This affinity of conjugated arylidene ketones for thiols, in contrast to other functional groups present in nucleic acids, indicates that the genotoxic properties displayed by various contemporary anticancer drugs[6] should be absent in these compounds. Furthermore, a number of different proteins contain thiol groups, leading to the possibility that these compounds have multiple molecular targets. The importance of such pleiotropy has recently been discussed.[7–9] Currently, emphasis has been placed on the inclusion of a 1,5-diaryl-3-oxo-1,4-pentadienyl group (ARCH=CHCOCH=CHAR), referred to hereafter as a dienone moiety, into candidate cytotoxins. This pharmacophore presents the possibility that sequential thiol alkylation can occur with the olefinic carbon atoms. Multiple studies have revealed that an initial lowering of the concentration of cellular thiols, followed by a second chemical attack, is more detrimental to malignant cells than normal tissues.[10,11] In addition, if this interaction occurs at two different sites, the effect may be far more detrimental to the neoplasm than reaction at only one site.[12]

The aim of the present investigation was to evaluate the hypothesis of cytotoxic synergism in cancer cells, which suggests that compounds capable of multiple cellular interactions in neoplasms exert a synergistic effect. In order to probe the viability of this theory, we designed a series of compounds (**1**) containing two dienone groups (Figure 1). In this case, the inclusion of two such groups into a molecule may more than double the potency of a related compound containing only one dienone moiety. Series **1** was designed to include compounds in which the locations of the dienone groups vary in

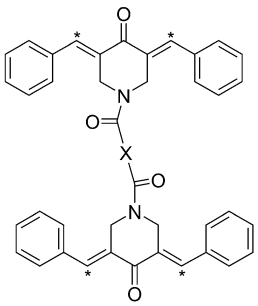

1

Figure 1. General structure of series **1**. * indicates the olefinic carbon atoms that are capable of interacting with different thiol groups of a protein.

[a] *S. Das, Dr. U. Das, Prof. Dr. D. K. J. Gorecki, Prof. Dr. J. R. Dimmock*
Drug Design & Discovery Research Group, College of Pharmacy & Nutrition, University of Saskatchewan
216 Thorvaldson, 110 Science Place, Saskatoon, Saskatchewan S7N 5C9 (Canada)
E-mail: jr.dimmock@usask.ca

[b] *Dr. A. Varela-Ramírez, Dr. C. Lema, Prof. Dr. R. J. Aguilera*
Cell Culture & High-Throughput Screening Facility, Border Biomedical Research Center&Department of Biological Sciences, University of Texas at El Paso, 500 West University Avenue, El Paso, Texas 79968-0519 (USA)

[c] *Prof. Dr. J. Balzarini, Prof. Dr. E. D. Clercq*
Rega Institute of Medical Research, Katholieke Universiteit Leuven
Minderbroedersstraat 10, 3000 Leuven (Belgium)

[d] *Prof. Dr. S. G. Dimmock*
Department of Finance, Nanyang Technological University
S3-B1A-02, 100 Nanyang Avenue, 639798 (Singapore)

Supporting information for this article is available on the WWW under http://dx.doi.org/10.1002/cmdc.201100199.

relation to each other. Molecular modeling was used as a means to determine the spatial relationship between the pharmacophores. Biological evaluations were undertaken using multiple cell lines in order to explore the generality of any trends in the relative potencies of the compounds.

Results

Compounds were synthesized using the procedure indicated in Scheme 1. All of the compounds in series **1** were evaluated against human Molt 4/C8 and CEM T-lymphocytes, as well as murine L1210 cells (Table 1). Various structural features of **1a**–**j** were examined by molecular modeling. The most active compounds, **1a** and **1b**, were evaluated against a large number of human tumor cell lines, and selected biological data from these studies is presented in Figure 4. In general, lead compound **1a** displayed greater potency toward non-adherent cells than toward either an adherent neoplasm or two fibroblasts. These results are illustrated in Figures 5 and 6 and Table 3. Cell-cycle analysis of **1a** revealed that this compound resulted in apoptosis in four neoplastic cell lines, and necrosis was also observed (Figure 7).

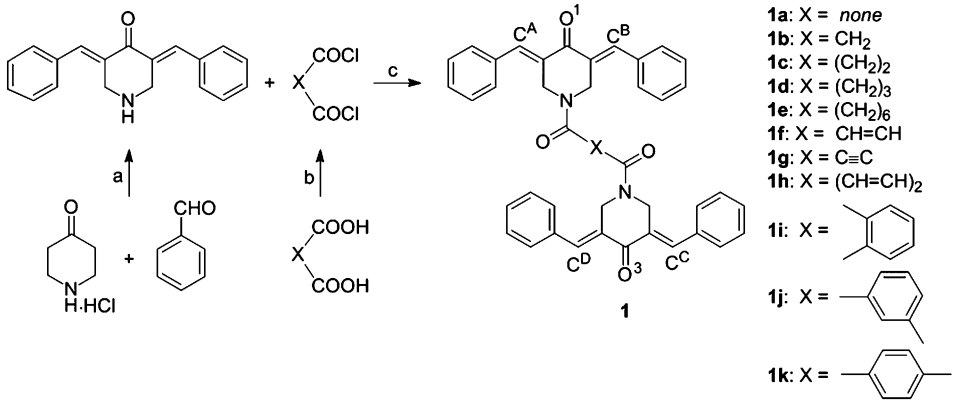

Scheme 1. Synthesis of series **1**. *Reagents and conditions*: a) AcOH, dry $HCl_{(g)}$, 10% aq K_2CO_3, RT, 12 h, 80%; b) $SOCl_2$, 60–65 °C, 4–5 h, 90%; c) Et_3N, ~20 °C, 12 h, 48–72%.

Discussion

^{1}H NMR spectra of **1a**–**k** indicate that the compounds are stereoisomerically pure, and absorbance of the olefinic protons in the region from 7.63–7.90 ppm indicates that the compounds have an *E* configuration.[13] In addition, X-ray crystallography of a number of 3,5-bis(benzylidene)-4-piperidones also confirmed that these compounds adopt the *E* stereochemistry.[13,14] While this study was in progress, syntheses of 2-fluoro analogues of **1a** and **1f** were described, and X-ray crystallography of the 2-fluoro analogue of **1a** showed that the four olefinic double bonds possess an *E* configuration.[15]

The compounds in series **1** were evaluated against human Molt 4/C8 and CEM T-lymphocytes in order to determine whether they demonstrate cytotoxic properties towards human transformed cells. A murine L1210 assay was employed, as a number of anticancer drugs display potency in this screen,[16] and it may, therefore, identify compounds of potential clinical value. The results presented in Table 1 show that a number of compounds in series **1** are potent cytotoxins. However, compound **1k** is virtually insoluble in multiple solvents, and the observed IC_{50} values of greater than 500 μM in the three assays is likely due to the insufficient solubility of **1k** in the media preventing penetration of the malignant cells. Hence, this compound has been removed from further discussion of the correlations between series **1** compounds and cytotoxic potencies. With regard to the IC_{50} values of **1a**–**j**, 47% are more potent than melphalan, 60% are below 5 μM, and six are in the sub-micromolar range. Of particular interest are **1a** and **1b**, which have average IC_{50} values towards Molt 4/C8 and CEM T-lymphocytes of 0.61 and 0.14 μM, respectively, and clearly emerge as lead molecules. The following compounds have IC_{50} values that indicate higher potency than melphalan, which is an alkylating agent used in cancer chemotherapy (the fold increase in relative potency as com-

Table 1. Evaluation of **1a**–**j** against Molt 4/C8, CEM, and L1210 cells, as well as a comparison of their potencies with **2**.[a]

Compd	Molt 4/C8 cells		CEM cells		L1210 cells	
	IC_{50} [μM]	RP[b]	IC_{50} [μM]	RP[b]	IC_{50} [μM]	RP[b]
1a	0.46±0.11	18	0.75±0.16	2.5	4.46±0.23	1.8
1b	0.07±0.01	115	0.20±0.17	9.3	1.23±0.38	6.5
1c	0.57±0.16	14	1.21±0.87	1.5	14.0±1.2	0.6
1d	1.61±0.05	5.0	2.03±0.48	0.9	11.5±0.3	0.7
1e	1.53±0.54	5.3	2.28±0.27	0.8	15.3±4.2	0.5
1f	4.40±2.95	1.8	7.75±0.07	0.2	28.9±2.0	0.3
1g	1.50±0.10	5.4	3.35±1.27	0.6	9.86±0.76	0.8
1h	25.1±15.8	0.3	39.2±5.4	0.1	79.0±10.2	0.1
1i	0.85±0.41	9.5	1.45±0.85	1.3	4.19±2.19	1.9
1j	12.5±1.8	0.7	36.0±7.6	0.1	150±65	0.1
2	8.07±0.45	–	1.86±0.08	–	7.97±0.75	–
Melphalan	3.24±0.79	–	2.47±0.30	–	2.13±0.03	–

[a] IC_{50} values were determined using a literature procedure and are the average of three independent experiments ±SD. [24] Cells were exposed to the compounds for 3 d (Molt 4/C8 and CEM screens) or 2 d (L1210 assay). [b] Relative potencies (RP) were obtained by dividing the IC_{50} values of **2** by the values for each of the compounds in series **1**.

pared with melphalan is given in parentheses): **1a** (7.0), **1b** (44), **1c** (5.7), **1d** (2.1), **1g** (2.2), and **1i** (3.8) in the Molt 4/C8 screen; **1a** (3.3), **1b** (12), and **1c** (2.0) in the CEM test; **1b** (1.7) towards L1210 cells.

For **1a–j**, IC_{50} values are lowest in the Molt 4/C8 screen and highest in the L1210 assay. This observation is confirmed by average IC_{50} values for **1a–j** in the Molt 4/C8, CEM, and L1210 tests of 4.86, 9.42, and 31.8 μM, respectively (Table 1). Variations in potency were displayed by each compound **1a–j** towards Molt 4/C8, CEM, and L1210 cells. For example, Molt 4/C8 T-lymphocytes are 25-times more sensitive to treatment with **1c** than are L1210 cells, and this differential toxicity may be also be observed between malignant and non-malignant cells, leading to greater adverse effects toward neoplasms.

The following observations were made pertaining to the effect of the nature of the spacer group (X in structure **1**) on average IC_{50} values of **1a–j** towards T-lymphocytes (these values are given in parentheses). The most potent compound is **1b** (0.14 μM) which has a single methylene group spacer. Removal of the spacer, leading to **1a** (0.61 μM), or insertion of additional methylene groups to **1b**, giving rise to **1c** (0.89 μM), **1d** (1.82 μM), and **1e** (1.91 μM), led to reduced potencies. A comparison of IC_{50} values for three compounds which have a two carbon atom spacer showed that **1f** (6.08 μM) and **1g** (2.43 μM) are less potent than **1c** (0.89). The addition of a further olefinic linkage to **1f** (6.08 μM), creating **1h** (32.2 μM), reduced potency five-fold. Upon introduction of an aryl ring spacer, the relative location of the substituents influences potency considerably, as observed by the substantial difference in IC_{50} values for **1c** (1.15 μM) and **1j** (24.3 μM).

If the hypothesis is valid that synergism occurs when each compound interacts at a different binding site, then one would expect to observe similar relative potencies using various biological assays. In order to evaluate this possibility, Kendall's coefficient of concordance[17] was applied to data generated in our three assays. Equation (1) used in this determination is given below, where W is Kendall's coefficient of concordance, i denotes the individual compound ($i=1$ for **1a**, $i=2$ for **1b**, etc.), n is the number of compounds, R_i is the average rank given to cell line i, m is the number of cell lines, T is the correction factor for ties and j refers to the individual cell line. Kendall's coefficient of concordance is a test for assessing the similarity of rankings. If the relative potency rank for each assay is identical, Kendall's coefficient of concordance will be 1. If there is no agreement in rankings, Kendall's coefficient of concordance will be zero. The coefficient of concordance for our biological data was found to be 0.924 ($p=0.03$), providing very strong evidence that the relative potency rankings are similar across the assays. One may conclude, therefore, that despite the difference in sensitivity of the three cell lines to **1a–j**, the molecular shapes may influence cytotoxic potencies in a similar fashion.

$$W = \frac{12\sum_{i=1}^{n}\left(R_i^2\right) - 3m^2n(n+1)^2}{m^2n(n^2-1) - m\sum_{j=1}^{m}\left(T_j\right)} \quad (1)$$

The hypothesis that synergism may occur with the presence of two dienone groups was examined by comparing the IC_{50} values of **1a–j** with that of piperidone **2**. This dienone was chosen because, like the compounds in series **1**, **2** is a 1-acyl-3,5-bis(benzylidene)-4-piperidone. Additionally, the hydrophobic 1-tetradecanoyl group ensures that **2** resembles series **1** with regard to their markedly lipophilic nature. For example, the log*P* values of **1e** and **2** are 8.58 and 9.02, respectively. If the hypothesis of cytotoxic synergism is valid, then the cytotoxic potencies of **1a–j** should be greater than twice the figures generated for **2**. Therefore, the IC_{50} value of **2** was divided by the corresponding value for each of analogues **1a–j** in the Molt 4/C8, CEM, and L1210 assays to give the relative potency (RP) figures (Table 1). RP values greater than two were obtained for **1a–e, g**, and **i** in the Molt 4/C8 screen, **1a** and **b** in the CEM assay, and **1b** in the L1210 test, that is, in one-third of the comparisons made. The RP figures for the Molt 4/C8 screen are particularly encouraging, and these results warrant further evaluation of the hypothesis.

Previous studies by our group involved the evaluation of several series of structurally related 1-acyl-3,5-bis(benzylidene)-4-piperidones for cytotoxic properties, including assessment using Molt 4/C8, CEM, and L1210 cells. Series **3–5** have, respectively, aroyl,[18] acryloyl,[13] and phosphono[19] groups attached to the nitrogen atom (Figure 2). In general, series **1** exhibits

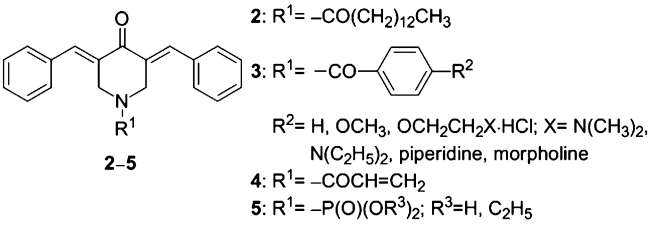

Figure 2. Structures of compounds in series **2–5**.

slightly weaker activities than **3–5**; however, removal of the two outliers (**1h** and **1j**) shows that the observed IC_{50} values for the remaining members of the series are comparable to series **3–5** (Table 2).

Further evaluation of the biological data presented in Table 1 was undertaken in order to examine the theory that the topography of **1a–j** controls cytotoxicity. While a substantial number of interatomic distances as well as various bond

Table 2. Potencies of series **1** compounds as compared to series **3–5**.

Compd	IC_{50}[a] [μM] Molt 4/C8	CEM	L1210
3	2.64	2.92	49.8
4[b]	1.42	1.48	8.69
5	0.91	1.70	7.33
1a–j	4.86	9.42	31.8
1a–g,i	1.37	2.38	11.2

[a] Values shown are the average of three independent experiments. [b] Data reported previously.[13]

and torsion angles could be determined, we focused primarily on the relative positions of the olefinic carbon atoms of both pharmacophores, followed by the piperidyl nitrogen atoms and the spacer group oxygen atoms. The generated figures are presented in table S1 of the Supporting Information.

The relative positions of the olefinic carbon atoms in both pharmacophoric groups were determined as follows: The four olefinic carbon atoms were designated C^A, C^B, C^C, and C^D (Figure 3a). Axes 1 and 2 were constructed (Figure 3b), and d_1, d_2, and ψ were measured. Linear and semi-logarithmic plots were generated using the average IC_{50} values of **1a–j** towards Molt 4/C8 and CEM T-lymphocytes and their d_1, d_2, and ψ data. No correlations ($p > 0.05$) nor trends to significance ($p > 0.1$) were found, although a negative trend to significance was nearly attained when using ψ values ($p = 0.11$). Thus, the possibility exists that the preparation of analogues of series **1** in which ψ values are increased may lead to molecules with greater cytotoxicity. Linear and semi-logarithmic plots were constructed using the average IC_{50} values of **1a–j** towards the two T-lymphocyte cell lines and the interatomic distances d_3 (N1—N2), d_4 (N1—O2) and d_5 (O2—O4) (Figure 3c). Positive correlations were noted between the IC_{50} values and d_3 ($p = 0.04$), d_4 ($p = 0.04$), and d_5 ($p = 0.02$), indicating that potency increases as the d_3–d_5 spans diminish. Expansion of this project should involve the design of molecules in which the spacer group (X) is either small or eliminated entirely. In addition, these results highlight the importance of the proximity of the piperidyl nitrogen atoms to the oxygen atoms. Further experimentation should be pursued, such as incorporating the CO—X—CO group into rigid heterocyclic rings with the goal of finding the optimal topography of these molecules to maximize cytotoxic properties.

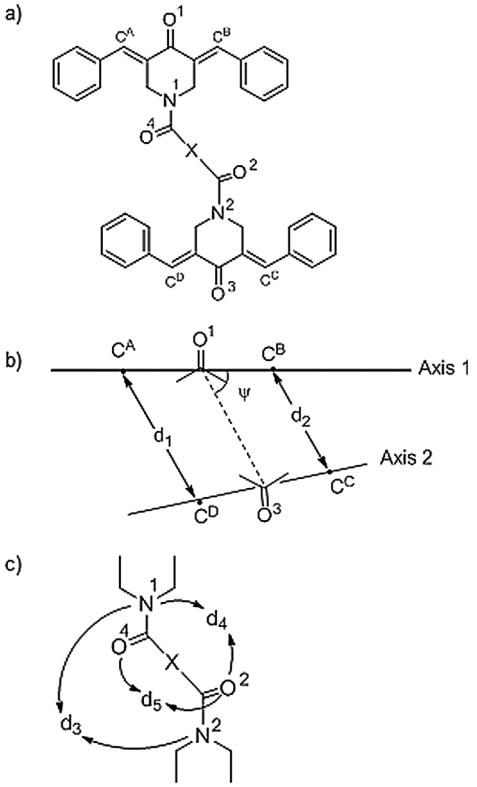

Figure 3. Various structural features of **1a–j** as determined by molecular modeling: a) olefinic carbon atoms C^A–C^D, piperidyl nitrogen atoms N1 and N2, and carbonyl oxygen atoms O1–O4; b) interatomic distances d_1 and d_2, and bond angle ψ; and c) interatomic distances d_3–d_5.

In light of the encouraging biological data displayed by **1a–g**, and **i**, we undertook further evaluations. First, it was necessary to select a lead compound. As shown in Table 1, both **1a** and **1b** exhibited sub-micromolar IC_{50} values toward human cancer cells. These molecules were, therefore, evaluated against a substantial number of human tumor cell lines,[20] with the cytotoxic effect of **1a** and **1b** against some of these neoplasms presented in Figure 4. The data presented shows that **1a** generally displays lower IC_{50} values than **1b**; consequently, **1a** was chosen for further studies. An additional noteworthy feature of **1a** and **1b** is the differential potencies both compounds display towards the cell lines. This observation strengthens the view expressed earlier that these compounds and analogues in series **1** may possess greater toxicity towards neoplasms than normal cells.

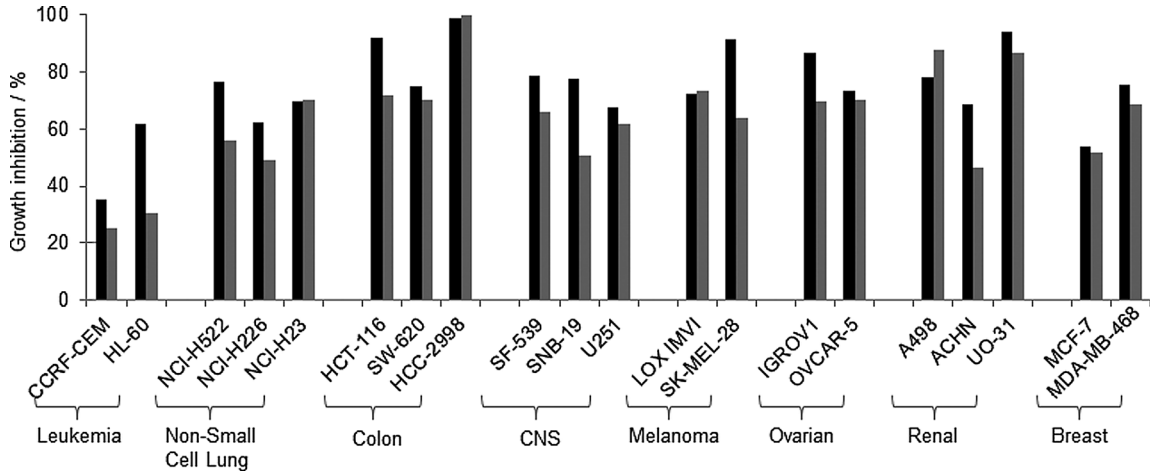

Figure 4. Growth inhibitory effect of 10 μM **1a** or **1b** toward a number of human tumor cell lines. Cells were exposed to **1a** (■) and **1b** (■) for 48 h using a previously described procedure.[20]

The ability of non-adherent cells to diffuse in vivo, leading to metastasis, led us to next address the discovery of novel prototypic molecules that inhibit the growth of non-adherent neoplasms. The potential of such compounds would be enhanced even further if greater toxicity could be demonstrated towards non-adherent neoplasms over either adherent or non-malignant cells. Compound **1a** was examined against the following non-adherent cell lines: human CEM, JURKAT, and SUP-T1 and murine EL-4 T-cell lymphomas, as well as human BJAB, Nalm-6, and Ramos B-cell lymphomas. This compound was also assessed against adherent human HeLa ovarian cancer cells, as well as two adherent non-malignant cell lines: human foreskin Hs27 and murine N1H-3T3 fibroblasts.

Figure 5 shows that, in general, greater toxicity was demonstrated toward non-adherent cells than toward either the adherent HeLa cell line or the two fibroblasts. CC_{50} values were

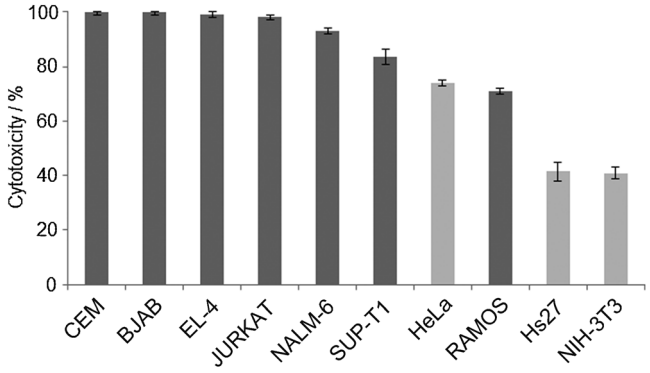

Figure 5. Cytocidal effects of **1a** (5 μM) as determined by flow cytometry using a previously reported method.[25] Cells are non-adherent with the exception of the adherent HeLa, Hs27, and N1H-3T3 cell lines. Each bar represents the average value of triple measurements with error bars showing standard deviations. Cells were exposed to **1a** for 22 h.

also determined in order to garner an appreciation of the differential toxicity between several non-adherent cells and the adherent NIH-3T3 fibroblast (Table 3). Selectivity index values are impressive and establish **1a** as an important lead molecule. Further experimentation was initiated to determine whether higher toxicity toward non-adherent over adherent cell lines is a common property of the more potent compounds in series **1**. Accordingly, **1b**–**g**, and **i** were evaluated against JURKAT and SUP-T1 non-adherent cells, as well as against normal (Hs27) and malignant (HeLa) adherent cell lines (Figure 6). The various

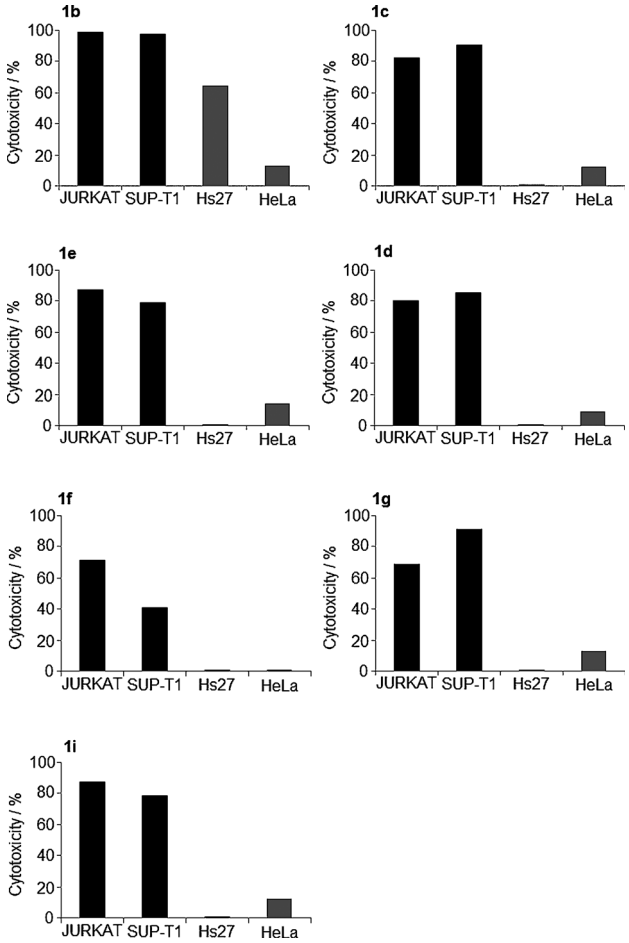

Figure 6. Evaluation of **1b**–**g**, and **1i** against non-adherent (JURKAT, SUP-T1) and adherent (Hs27, HeLa) cells. Concentrations of compounds used were 2.5 μM (**1f**, **g**, and **i**), 5 μM (**1e**), and 10 μM (**1b**–**d**). Cells were exposed to compounds for 22 h as previously described.[25]

Table 3. Evaluation of **1a** against non-adherent cell lines and NIH-3T3 fibroblasts.

Cell line	CC_{50}[a] [μM]	SI[b]
CEM	0.034	376
EL-4	0.031	412
JURKAT	0.029	441
Nalm6	0.022	581
Sup-T1	0.384	33
NIH-3T3	12.78	–

[a] Cells were incubated with **1a** for 22 h as previously described.[25] Values shown are the average of three independent experiments. [b] Selectivity index (SI) figures are quotients of the CC_{50} values of **1a** toward NIH-3T3 fibroblasts and the data for each of the non-adherent cell lines.

concentrations of **1b**–**g** and **i** were chosen to emphasize the consistently greater cytotoxicity of these compounds in adherent versus non-adherent cells. The results provide unequivocal evidence that **1b**–**g** and **i**, similar to **1a**, display preferential toxicity against non-adherent cells. This observation strengthens the need for development of these compounds, which display antimetastatic potential in addition to their cytotoxic properties.

Flow cytometry was pursued, using four non-adherent cell lines, in order to gain an understanding of the ways in which **1a** mediates its cytotoxic properties (Figure 7). After 8 h incubation, an average of 19% of the cells were apoptotic, with this percentage doubling after 20 h. Necrosis was virtually absent after 8 h, while on an average of 9% of the cells were necrotic after 20 h. One may therefore conclude that **1a** causes cell death inter alia by apoptosis and, to a lesser

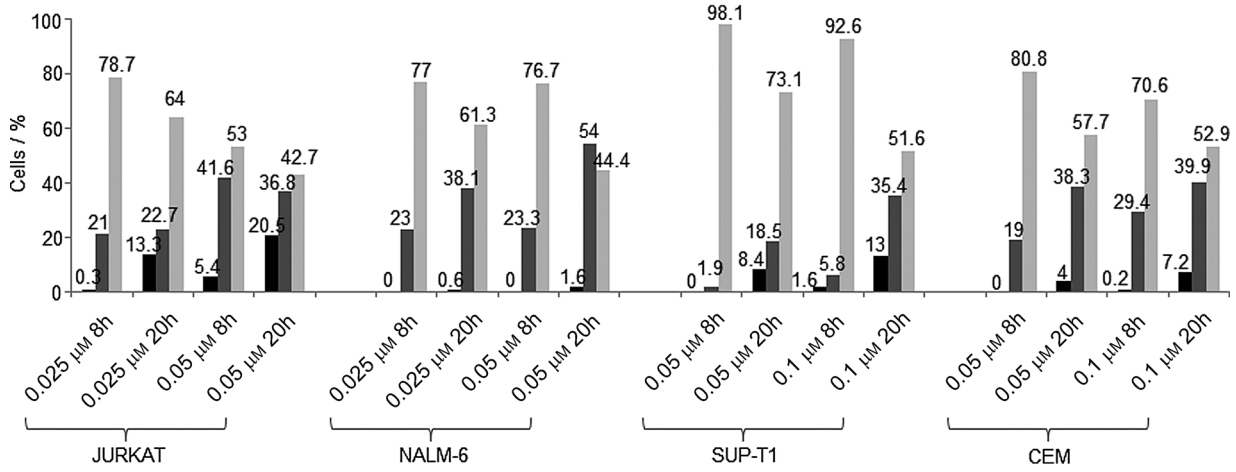

Figure 7. Flow cytometry analysis of the cytotoxic effect of **1a** on four non-adherent cell lines following incubation for 8 and 24 h.[25] The exact percentage of apoptotic (■), necrotic (■), and viable (■) cells is indicated at the top of each bar graph. Two concentrations of **1a** are shown on the x-axis. Note that two-fold higher concentrations were utilized for the most resistant cell lines, SUP-T and CEM.

degree, by necrosis. In a previous study, a cytotoxic 1-acyl-3,5-bis(benzylidene)-4-piperidone activated caspase-3, with the extent of activation dependent on the cell line under investigation.[21] Since caspases are involved in most apoptosis, it is likely that one mechanism by which **1a–j** may exert their cytotoxic properties is the activation of one or more caspases.

Conclusions

This study reveals that the unsaturated ketones in series **1** are, in general, potent cytotoxins. The theory that increasing the number of sites for thiol alkylation two-fold should more than double cytotoxic potency was validated in approximately half of the biological data generated using Molt 4/C8 and CEM T-lymphocytes, although there was little support when utilizing the murine L1210 screen. Extensions of this study should consider the design and evaluation of analogues of **1a–j** that contain more than two identical phamacophores. In addition, the synthesis of heterodimers should be pursued in which different substituents are appended to the aryl rings, thereby creating molecules with varying atomic charges on the olefinic carbon atoms. For compounds such as these, stepwise reactions with thiols should be enhanced, which may lead to greater increases in toxicity to neoplasms than to normal cells.[10,11] Molecular modeling was also used to emphasize the importance of the relative positions of the amide groups.

From this initial investigation, **1a** and **1b** emerged as lead molecules, displaying potent cytotoxicity against a wide range of human tumor cell lines. Further evaluations using **1a** revealed its increased toxicity toward non-adherent cell lines than toward either an adherent neoplasm or fibroblasts. Compound **1a** was shown to exert its toxic effects against certain cancer cells through apoptosis and necrosis. Sufficient evidence has been presented through these studies to warrant rapid expansion of evaluation of this compound series in order to further investigate their potential as candidate anticancer agents.

Experimental Section

Chemistry

Synthesis of 1a–k: Melting points were determined on a Gallenkamp instrument and are uncorrected. ^{1}H and ^{13}C NMR spectra were obtained using a Bruker Avance AMX 500 spectrometer equipped with a BBO probe. Chemical shifts (δ) are reported in ppm. Mass spectra were obtained using a quad tandem 4000 QTRAP mass analyzer. Elemental analyses were undertaken using a CHNS elemental analyzer (Vario EL III microanalyzer).

General procedure for the synthesis of 3,5-bis(benzylidene)-4-piperidone dimers (1a–k): A mixture of the corresponding dicarboxylic acid (0.005 mol) and thionyl chloride (0.02 mol, 2.4 g) was heated at 60–65 °C for 4–5 h. Excess thionyl chloride was removed at 45 °C in vacuo and moisture-free conditions. The resulting acid chloride was used for further reaction without purification.

The previously prepared acid chloride in 1,2-dichloroethane (DCE; 5 mL) was added slowly over a period of 30 min to a stirred suspension of 3,5-bis(benzylidene)-4-piperidone (0.009 mol, 2.75 g) prepared according to a literature method[13] in DCE (20 mL) containing Et_3N (0.11 mol, 1.12 g) at ≈20 °C. The reaction stirred at RT overnight, then the solvent was removed in vacuo at 45 °C. Aq K_2CO_3 (25 mL, 10% *w/v*) was added to the crude material and stirred for 2 h. The resulting solid was filtered, dried, and crystallized from a suitable solvent to yield pure product. In the case of **1a**, **b**, **d**, and **e**, the appropriate acid chlorides were procured from commercial sources.

1,2-Bis(3,5-dibenzylidene-4-oxo-piperidin-1-yl)ethane-1,2-dione (1a): Yield: 62%; mp: 246 °C ($CHCl_3$/MeOH); ^{1}H NMR (500 MHz, [D_6]DMSO): δ = 7.72 (s, 2H, 2×=CH), 7.56 (s, 2H, 2×=CH), 7.53 (t, 4H, Ar-H), 7.49 (d, J = 7.07 Hz, 2H, Ar-H), 7.45 (m, 6H, Ar-H), 7.39 (m, 8H, Ar-H), 4.48 ppm (d, J = 23.28 Hz, 8H, 4×NCH_2); ^{13}C NMR (125 MHz, [D_6]DMSO): δ = 184.7, 162.6, 137.9, 137.5, 134.4, 134.1, 131.4, 131.0, 130.9, 130.7, 130.2, 130.1, 129.3, 129.2, 46.4, 41.6 ppm; MS (ESI) *m/z*: 627 $[M+Na]^+$; Anal. calcd for $C_{40}H_{32}N_2O_4 \cdot H_2O$: C 77.17; H 5.14; N 4.50, found: C 77.05; H 4.87; N 4.42.

1,3-Bis-(3,5-dibenzylidene-4-oxo-piperidin-1yl)propane-1,3-dione (1b): Yield: 65%; mp: 201 °C (acetone); ^{1}H NMR (500 MHz, [D_6]DMSO): δ = 7.72 (s, 2H, 2×=CH), 7.57 (s, 2H, 2×=CH), 7.53 (d,

J=4.18 Hz, 8H, Ar-H), 7.47 (m, 12H, Ar-H), 4.62 (d, J=21.13 Hz, 8H, 4×NCH_2), 3.46 ppm (s, 2H, CH_2); ^{13}C NMR (125 MHz, [D_6]DMSO): δ=186.3, 165.9,136.6, 136.5, 134.7, 134.5, 132.6, 132.5, 131.0, 130.9, 130.1, 130.0, 129.3, 129.2, 47.0, 42.4 ppm; MS (ESI) m/z: 641 [M+Na]$^+$; Anal. calcd for $C_{41}H_{34}N_2O_4{\cdot}H_2O$: C 77.27; H 5.65; N 4.39, found: C 77.31; H 5.50; N 4.47.

1,4-Bis-(3,5-dibenzylidene-4-oxo-piperidin-1-yl)butane-1,4-dione (1c): Yield: 58%; mp: 188 °C ($CHCl_3$/MeOH); ^1H NMR (500 MHz, [D_6]DMSO): δ=7.68 (s, 4H, 4×=CH), 7.49 (m, 20H, Ar-H), 4.78 (d, J=10.95 Hz, 8H, 4×NCH_2), 2.29 ppm (s, 4H, 2×CH_2); ^{13}C NMR (125 MHz, [D_6]DMSO): δ=186.5, 170.4, 136.6, 136.5, 134.8, 134.5, 133.0, 132.8, 131.0, 130.0, 129.3, 46.3, 42.9, 27.16 ppm; MS (ESI) m/z: 655 [M+Na]$^+$; Anal. calcd for $C_{42}H_{36}N_2O_4{\cdot}0.5H_2O$: C 78.53; H 5.76; N 4.36, found: C 78.16; H 5.71; N 4.11.

1,5-Bis-(3,5-dibenzylidene-4-oxo-piperidin-1-yl)pentane-1,5-dione (1d): Yield: 43%; mp: 170 °C ($CHCl_3$/MeOH); ^1H NMR (500 MHz, [D_6]DMSO): δ=7.71 (s, 2H, 2×=CH), 7.66 (s, 2H, 2×=CH), 7.54 (m, 14H, Ar-H), 7.42 (m, 6H, Ar-H), 4.76 (d, 8H, 4×NCH_2, J=28.18 Hz), 2.02 (t, 4H, 2×CH_2), 1.42 ppm (p, 2H, CH_2); ^{13}C NMR (125 MHz, [D_6]DMSO): δ=186.6, 171.0, 136.6, 134.8, 134.5, 133.1, 133.0, 131.0, 130.3, 129.3, 46.4, 42.8, 31.3, 20.4 ppm; MS (ESI) m/z: 627 [M+Na]$^+$; Anal.calcd for $C_{43}H_{38}N_2O_4{\cdot}0.25H_2O$: C 79.22; H 5.91; N 4.30, found: C 79.18; H 5.64; N 4.08.

1,8-Bis-(3,5-dibenzylidene-4-oxo-piperidin-1-yl)octane-1,8-dione (1e): Yield: 64%; mp: 160 °C ($CHCl_3$/MeOH); ^1H NMR (500 MHz, [D_6]DMSO): δ=7.71 (s, 4H, 4×=CH), 7.51 (m, 20H, Ar-H), 4.81 (d, 8H, J=29.13 Hz, 4×NCH_2), 2.00 (t, 4H, 2×CH_2), 1.20 (m, 4H, 2×CH_2), 0.76 ppm (m, 4H, 2×CH_2); ^{13}C NMR (125 MHz, [D_6]DMSO): δ=186.6, 171.4, 136.8, 136.4, 134.8, 134.6, 133.2, 131.0, 130.0, 129.3, 46.5, 43.1, 32.4, 28.5, 24.7 ppm; MS (ESI) m/z: 711 [M+Na]$^+$; Anal.calcd for $C_{46}H_{44}N_2O_4{\cdot}0.5H_2O$: C 79.10; H 6.30; N 4.01, found: C 78.85; H 6.32; N 4.04.

1,4-Bis-(3,5-dibenzylidene-4-oxo-piperidin-1-yl)but-2-ene-1,4-dione (1f): Yield: 71%; mp: 220 °C (EtOH); ^1H NMR (500 MHz, [D_6]DMSO): δ=7.74 (s, 2H, 2×=CH), 7.66 (s, 2H, 2×=CH), 7.51 (m, 20H, Ar-H), 6.92 (s, 2H, 2×=CH), 4.83 ppm (d, J=8.54 Hz, 8H, 4×NCH_2); ^{13}C NMR (125 MHz, [D_6]DMSO): δ=186.2, 163.9, 136.9, 136.7, 134.7, 134.3, 132.6, 131.0, 130.1, 129.3, 46.9, 43.1 ppm; MS (ESI) m/z: 653 [M+Na]$^+$; Anal.calcd for $C_{42}H_{34}N_2O_4{\cdot}5H_2O$: C 69.92; H 4.71; N 3.88, found: C 69.85; H 4.79; N 3.57.

1,4-Bis-(3,5-dibezylidene-4-oxo-piperidin-1-yl)-but-2-yne-1,4-dione (1g): Yield: 48%; mp: 220 °C ($CHCl_3$/MeOH; dec.); ^1H NMR (500 MHz, [D_6]DMSO): δ=7.81 (s, 1H, =CH), 7.75 (d, 2H, 2×=CH, J=17.63 Hz), 7.68 (s,1H, =CH), 7.56 (m,20H, Ar-H), 4.79 (d, J=18.80 Hz, 4H, 2×NCH_2), 4.64 ppm (d, J=16.96 Hz, 4H, 2×NCH_2); ^{13}C NMR (125 MHz, [D_6]DMSO): δ=186.0, 185.7, 185.4, 162.4, 161.9, 149.9, 137.2, 134.5, 132.3, 131.8, 131.5, 131.0, 130.7, 130.4, 129.1, 128.7, 125.25, 95.25, 46.8, 42.7, 42.2 ppm; MS (ESI) m/z: 651 [M+Na]$^+$; Anal.calcd for $C_{42}H_{32}N_2O_4{\cdot}2H_2O$: C 75.82; H 4.81; N 4.21, found: C 75.48; H 4.74; N 4.01.

1,6-Bis-(3,5-dibenzylidene-4-oxo-piperidin-1-yl)-hexa-2,4-diene-1,6-dione (1h): Yield: 56%; mp: 199 °C ($CHCl_3$/MeOH); ^1H NMR (500 MHz, $CDCl_3$): δ=7.87 (s, 4H, 4×=CH), 7.42 (m, 20H, Ar-H), 6.94 (m, 2H, 2×=CH), 6.16 (m, 2H, 2×=CH), 4.98 (s, 4H, 2×NCH_2), 4.77 ppm (s, 4H, 2×NCH_2); ^{13}C NMR (125 MHz, [D_6]DMSO): δ=186.6, 164.7, 140.3, 137.5, 134.5, 131.5, 130.6, 130.0, 125.9, 125.6, 46.3, 44.1 ppm; MS (ESI) m/z: 679 [M+Na]$^+$; Anal.calcd for $C_{44}H_{36}N_2O_4{\cdot}2.5H_2O$: C 75.23; H 5.12; N 3.98, found: C 75.23; H 5.02; N 3.91.

1,2-Bis-[(3,5-dibenzylidene-4-oxo-piperidin-1-yl)-1-carbonyl]benzene (1i): Yield: 68%; mp: 240 °C ($CHCl_3$/MeOH; dec.); ^1H NMR (500 MHz, [D_6]DMSO): δ=7.77 (s, 2H, 2×=CH), 7.69 (s, 2H, 2×=CH), 7.57 (t, 10H, Ar-H), 7.27 (brs, 5H, Ar-H), 7.18 (brs, 5H, Ar-H), 6.89 (m, 2H, Ar-H), 6.78 (m, 2H, Ar-H), 4.92 (brs, 4H, 2×NCH_2), 4.49 ppm (s, 4H, 2×NCH_2); ^{13}C NMR (125 MHz, [D_6]DMSO): δ=186.1, 167.9, 137.3, 136.5, 134.8, 133.8, 132.6, 131.1, 130.3, 129.8, 129.4, 129.0, 126.4, 47.8, 43.4 ppm; MS (ESI) m/z: 703 [M+Na]$^+$; Anal.calcd for $C_{46}H_{36}N_2O_4{\cdot}H_2O$: C 78.99; H 5.43; N 4.0, found: C 79.09; H 5.42; N 4.02.

1,3-Bis-[(3,5-dibenzylidene-4-oxo-piperidin-1-yl)-1-carbonyl]benzene (1j): Yield: 63%; mp: 220 °C ($CHCl_3$/MeOH; dec.); ^1H NMR (500 MHz, [D_6]DMSO): δ=7.78 (s, 4H, 4×=CH), 7.53 (m, 10H, Ar-H), 7.31 (m, 10H, Ar-H), 7.11 (s, 1H, Ar-H), 7.06 (d, J=8.93 Hz, 2H, Ar-H), 6.75 (t,1H, Ar-H), 4.97 (brs, 4H, 2×NCH_2), 4.57 ppm (brs, 4H, 2×NCH_2); ^{13}C NMR (125 MHz, [D_6]DMSO): δ=186.03, 168.0, 137.2, 134.51, 132.6, 131.0, 130.1, 129.2, 128.9, 128.3, 125.7, 48.9, 45.6 ppm; MS (ESI) m/z: 703 [M+Na]$^+$; Anal.calcd for $C_{46}H_{36}N_2O_4{\cdot}0.5H_2O$: C 80.02; H 5.36; N 4.01, found: C 80.31; H 5.29; N 4.01.

1,4-Bis-[(3,5-dibenzylidene-4-oxo-piperidin-1-yl)-1-carbonyl]benzene (1k): Yield: 72%; mp: 220 °C (AcOH/H_2O; dec.); ^1H NMR (500 MHz, CF_3COOD): δ=10.44 (s, 2H, 2×=CH), 10.38 (s, 2H, 2×=CH), 9.81 (d, J=8.4 Hz, 10H, Ar-H), 9.63 (brs, 6H, Ar-H), 9.49 (brs, 4H, Ar-H), 9.16 (s, 4H, Ar-H), 7.47 (s, 4H, 2×NCH_2), 6.86 ppm (s, 4H, 2×NCH_2); ^{13}C NMR (125 MHz, CF_3COOD): δ=192.9, 174.1, 146.6, 144.2, 135.9, 135.4, 135.3, 133.4, 133.0, 132.6, 132.2, 132.0, 131.0, 130.9, 130.8, 129.0, 49.5, 47.12 ppm; Anal. calcd for $C_{46}H_{36}N_2O_4{\cdot}0.5H_2O$: C 80.02; H 5.36; N 4.01, found: C 79.67; H 5.25; N 3.99.

3,5-Bis(benzylidene)-1-tetradecanoyl-4-piperidone (2): Myristoyl chloride (0.011 mol, 2.7 g) in DCE (5 mL) was added slowly over a period of ≈30 min to a suspension of 3,5-bis(benzylidene)-4-piperidone (0.007 mol, 2 g), prepared according to a literature method,[13] in DCE (15 mL) containing Et_3N (0.016 mol, 1.7 gm) at ≈15 °C. The reaction stirred at RT overnight, then the solvent was removed in vacuo at 45 °C. Aq K_2CO_3 (25 mL, 10% w/v) was added to the crude, and the mixture was stirred for 2 h. The resulting solid was filtered, dried, and crystallized from EtOH. Yield: 90%; mp: 82 °C; ^1H NMR (500 MHz, $CDCl_3$): δ=7.91 (s, 1H, =CH), 7.85 (s, 1H, =CH), 7.53–7.40 (m, 10H, Ar-H), 4.96 (s, 2H, NCH_2), 4.87 (s, 2H, NCH_2), 2.14 (t, 2H, $COCH_2$), 1.45 (p, 2H, CH_2), 1.26 (m, 16H, Ar-H), 1.09 (m, 4H, 2×CH_2), 0.91 ppm (t, 3H, CH_3); ^{13}C NMR (125 MHz, $CDCl_3$): δ=186.9, 172.1, 138.6, 137.1, 134.7, 134.6, 132.1, 131.9, 130.7, 130.1, 129.6, 128.9, 128.8, 46.3, 43.6, 33.2, 32.0, 29.7, 29.7, 29.6, 29.5, 29.4, 29.3, 29.2, 25.1, 22.7, 14.2 ppm; Anal.calcd for $C_{31}H_{39}NO_2$: C 81.60; H 8.92; N 2.88, found: C 81.27; H 9.29; N 2.83.

Computational experiments

Molecular modeling: Models were built using the SYBYL 8.0 program[22] on a Lenovo workstation with the RHEL 4.0 operating system. Energy minimizations were performed with the conjugate gradient method using the Tripos force field and Gasteiger–Huckel charges with a convergence criterion of 0.001 kcal mol^{-1} Å. Each structure was further subjected to simulated annealing for identifying the lowest energy conformation. The system was heated at 1000 K for 1 ps, and then cooled at 200 K for 1 ps. The exponential annealing function was used, and ten such cycles were run. The lowest energy conformer was used to calculate the distance between two points and bond angles as depicted in Figure 3.

Determination of log P values: The predicted log *P* values for **1e** and **2** were obtained using Molinspiration Chemoinformatics software online.[23]

Biology

Cytotoxicity assays: The compounds in series **1** were evaluated against Molt 4/C8, CEM, and L1210 cells using a previously reported procedure.[24] Briefly, various concentrations of the compounds were incubated with the appropriate cell line in RPMI 1640 medium at 37 °C for 72 h (Molt 4/C8 and CEM assays) or 48 h (L1210 screen). Numbers of cells were determined using a Coulter counter. The IC_{50} value given is the concentration required to inhibit cell proliferation by 50%. Data are expressed as the mean ± SD from the dose–response curves of at least three independent experiments.

Compounds **1a** and **1b** were examined by the US National Cancer Institute against 52 and 59 human tumor cell lines, respectively, as previously described.[20] Solutions of 10^{-4}, 10^{-5}, 10^{-6}, 10^{-7} and 10^{-8} M of **1a** or **1b** were added to the cells, which were grown in RPMI 1640 medium containing 5% fetal bovine serum (FBS) and 2 mM L-glutamine. After incubation at 37 °C in an atmosphere of air (95%), carbon dioxide (5%), and relative humidity of 100% for 48 h, the concentration required to inhibit growth by 50% was determined spectrophotometrically using sulforhodamine B. Compound **1a** was evaluated at a concentration of 5 μM against CEM, BJAB, EL-4, JURKAT, Nalm-6, SUP-T1, HeLa, Ramos, Hs27, and N1H-3T3 cell lines essentially as previously described.[25] Briefly, a solution of **1a** in DMSO was added to cells grown in RPMI (CEM, BJAB, EL-4, JURKAT, Nalm6, SUP-T1 and Ramos) or DMEM (for HeLa, Hs27 and N1H-3T3) media, followed by incubation for 22 h at 37 °C. The average cytotoxicity of three independent experiments, expressed as a percentage, was obtained by noting the disruption of the plasma membrane using flow cytometry with propidium iodide as described previously.[25] In cases where 100% cytotoxicity is indicated, no cell viability was observed. Several of the 4-piperidones were also examined against JURKAT, SUP-T1, Hs27 and HeLa cells (concentration used, in μM, shown in parentheses): **1b** (10), **1c** (10), **1d** (10), **1e** (5), **1f** (2.5), **1g** (2.5), and **1i** (2.5). Using a range of concentrations of **1a**, we also obtained CC_{50} values of this compound towards JURKAT, SUP-T1, CEM, EL-4, Nalm6, and N1H-3T3 as previously described.[25]

*Flow cytometry analysis of **1a***: Compound **1a** was incubated with JURKAT, Nalm-6, SUP-T1, or CEM cells in RPMI media. After 8 and 20 h, the percentage of apoptotic, necrotic, and viable cells were determined by flow cytometry using Annexin-V-FITC and propidium iodide.[26]

Acknowledgements

*The authors thank the Canadian Institutes of Health for an operating grant to J.R.D. Appreciation is extended to the Belgian Concerted Research Actions (GoA 10/014) for providing funds to J.B. for the Molt 4/C8, CEM, and L1210 screens undertaken by L. van Berckelaer, and to the US National Cancer Institute for evaluating compounds **1a** and **1b** against a number of human tumor cell lines. This work was also supported by the Border Biomedical Research Center at the University of Texas at El Paso (USA) (5G12RR008124–16A1). B. McCullough and C. Sutton are thanked for their efforts in the preparation of this manuscript.*

Keywords: apoptosis · cytotoxic synergism · cytotoxicity · molecular modeling · unsaturated ketones

[1] J. R. Dimmock, L. M. Smith, P. J. Smith, *Can. J. Chem.* **1980**, *58*, 984 – 991.
[2] T. Aboul-Fodl, A.-N. El-Shorbagi, Z. A. Hozien, A.-W. Sarham, *Boll. Chim. Farm.* **2000**, *139*, 228 – 234.
[3] J. R. Dimmock, P. Kumar, M. Chen, J. W. Quail, J. Yang, T. M. Allen, G. Y. Kao, *Pharmazie* **1995**, *50*, 449 – 453.
[4] J. R. Dimmock, S. K. Raghavan, B. M. Logan, G. E. Bigam, *Eur. J. Med. Chem.* **1983**, *18*, 248 – 254.
[5] B. Mutus, J. D. Wagner, C. J. Talpas, J. R. Dimmock, O. A. Phillips, R. S. Reid, *Anal. Biochem.* **1989**, *177*, 237 – 243.
[6] E. X. Chen, M. J. Moore in *Principles of Medical Pharmacology*, 7th ed. (Eds: H. Kalant, D. M. Grant, J. Mitchell), Saunders – Elsevier, Toronto, **2007**, p. 778.
[7] L. M. Espinoza-Fonseca, *Bioorg. Med. Chem.* **2006**, *14*, 896 – 897.
[8] S. Frantz, *Nature* **2005**, *437*, 942 – 943.
[9] M. Galanski, B. K. Keppler, *Anti-Cancer Agents Med. Chem.* **2007**, *7*, 55 – 73.
[10] G. Chen, D. J. Waxman, *Biochem. Pharmacol.* **1994**, *47*, 1079 – 1087.
[11] K. Tsutsui, C. Komuro, K. Ono, T. Nishidai, Y. Shibamoto, M. Takahashi, M. Abe, *Int. J. Radiat. Oncol. Biol. Phys.* **1986**, *12*, 1183 – 1186.
[12] L. M. Chow, T. H. Chan, *Curr. Pharm. Des.* **2009**, *15*, 659 – 674.
[13] J. R. Dimmock, M. P. Padmanilayam, R. N. Puthucode, A. J. Nazarali, N. L. Motaganahalli, G. A. Zello, J. W. Quail, E. O. Oloo, H. B. Kraatz, J. A. Prisciak, T. M. Allen, C. L. Santos, J. Balzarini, E. De Clercq, E. K. Manavathu, *J. Med. Chem.* **2001**, *44*, 586 – 593.
[14] J. R. Dimmock, V. K. Arora, S. L. Wonko, N. W. Hamon, J. W. Quail, Z. Jia, R. C. Warrington, W. D. Fang, *Drug Des. Deliv.* **1990**, *6*, 183 – 194.
[15] P. Lagisetty, D. R. Powell, V. Awashthi, *J. Mol. Struct.* **2009**, *936*, 23 – 28.
[16] M. Suffness, T. Douros, in *Methods of Cancer Research, Volume XVI, Part A*; (Eds: V. T. De Vita, Jr., H. Busch) Academic Press, New York, **1979**, p. 84.
[17] D. Sheskin, *Handbook of Parametric and Nonparametric Statistical Procedures*, Chapman and Hall, London, **2004**, pp. 1093 – 1107.
[18] U. Das, J. Alcorn, A. Shrivastav, R. K. Sharma, E. De Clercq, J. Balzarini, J. R. Dimmock, *Eur. J. Med. Chem.* **2007**, *42*, 71 – 80.
[19] S. Das, U. Das, P. Selvakumar, R. K. Sharma, J. Balzarini, E. De Clercq, J. Molnár, J. Serly, Z. Baráth, G. Schatte, B. Bandy, D. K. J. Gorecki, J. R. Dimmock, *ChemMedChem* **2009**, *4*, 1831 – 1840.
[20] M. R. Boyd, K. D. Paull, *Drug Dev. Res.* **1995**, *34*, 91 – 109.
[21] U. Das, H. Sakagami, Q. Chu, Q. Wang, M. Kawase, P. Selvakumar, R. K. Sharma, J. R. Dimmock, *Bioorg. Med. Chem. Lett.* **2010**, *20*, 912 – 917.
[22] SYBYL 8.0, Tripos, St. Louis, MO.
[23] ACD/Labs release 10.00, version 10.02; http://www.acdlabs.com.
[24] P. G. Baraldi, M.Del. C. Nunez, M. A. Tabrizi, E. De Clercq, J. Balzarini, J. Bermejo, F. Estévez, R. Romagnoli, *J. Med. Chem.* **2004**, *47*, 2877 – 2886.
[25] B. T. Elie, C. Levine, I. Ubarretxena-Belandia, A. Varela-Ramírez, R. J. Aguilera, R. Ovalle, M. Contel, *Eur. J. Inorg. Chem.* **2009**, 3421 – 3430.
[26] N. Shaik, A. Martí, I. Augustin, H. Giovinazzo, A. Varela-Ramírez, M. Sanau, R. J. Aguilera, M. Contel, *Inorg. Chem.* **2009**, *48*, 1577 – 1587.

Received: April 18, 2011
Published online on August 8, 2011

